J|A|C|S
ARTICLES

Published on Web 07/29/2008

Rearrangement of the (6*S*,8*R*,11*S*) and (6*R*,8*S*,11*R*) Exocyclic 1,N^2-Deoxyguanosine Adducts of *trans*-4-Hydroxynonenal to N^2-Deoxyguanosine Cyclic Hemiacetal Adducts When Placed Complementary to Cytosine in Duplex DNA

Hai Huang, Hao Wang, Nan Qi, Albena Kozekova, Carmelo J. Rizzo, and Michael P. Stone*

Department of Chemistry and Center in Molecular Toxicology, Vanderbilt University, Nashville, Tennessee 37235

Received March 11, 2008; E-mail: michael.p.stone@vanderbilt.edu

Abstract: *trans*-4-Hydroxynonenal (HNE) is a peroxidation product of ω-6 polyunsaturated fatty acids. The Michael addition of deoxyguanosine to HNE yields four diastereomeric exocyclic 1,N^2-dG adducts. The corresponding acrolein- and crotonaldehyde-derived exocyclic 1,N^2-dG adducts undergo ring-opening to N^2-dG aldehydes, placing the aldehyde functionalities into the minor groove of DNA. The acrolein- and the 6*R*-crotonaldehyde-derived exocyclic 1,N^2-dG adducts form interstrand N^2-dG:N^2-dG cross-links in the 5′-CpG-3′ sequence context. Only the HNE-derived exocyclic 1,N^2-dG adduct of (6*S*,8*R*,11*S*) stereochemistry forms interstrand N^2-dG:N^2-dG cross-links in the 5′-CpG-3′ sequence context. Moreover, as compared to the exocyclic 1,N^2-dG adducts of acrolein and crotonaldehyde, the cross-linking reaction is slow (Wang, H.; Kozekov, I. D.; Harris, T. M.; Rizzo, C. J. *J. Am. Chem. Soc.* **2003**, *125*, 5687−5700). Accordingly, the chemistry of the HNE-derived exocyclic 1,N^2-dG adduct of (6*S*,8*R*,11*S*) stereochemistry has been compared with that of the (6*R*,8*S*,11*R*) adduct, when incorporated into 5′-d(GCTAGCXAGTCC)-3′•5′-d(G-GACTCGCTAGC)-3′, containing the 5′-CpG-3′ sequence (X = HNE-dG). When placed complementary to dC in this duplex, both adducts open to the corresponding N^2-dG aldehydic rearrangement products, suggesting that the formation of the interstrand cross-link by the exocyclic 1,N^2-dG adduct of (6*S*,8*R*,11*S*) stereochemistry, and the lack of cross-link formation by the exocyclic 1,N^2-dG adduct of (6*R*,8*S*,11*R*) stereochemistry, is not attributable to inability to undergo ring-opening to the aldehydes in duplex DNA. Instead, these aldehydic rearrangement products exist in equilibrium with stereoisomeric cyclic hemiacetals. The latter are the predominant species present at equilibrium. The *trans* configuration of the HNE H6 and H8 protons is preferred. The presence of these cyclic hemiacetals in duplex DNA is significant as they mask the aldehyde species necessary for interstrand cross-link formation.

Introduction

trans-4-Hydroxynonenal (**1**, HNE) is produced from the metabolism of membrane lipids,[1] and it is the major in vivo peroxidation product of ω-6 polyunsaturated fatty acids.[2,3] Several routes for the formation of HNE from ω-6 polyunsaturated fatty acids have been described.[4–6] HNE exhibits a range of biological effects, from alteration in gene expression and cell signaling to cell proliferation and apoptosis.[7–13] Human exposure to HNE has been implicated in the etiologies of a number of diseases associated with oxidative stress, including Alzheimer's disease,[14] Parkinson's disease,[15] arteriosclerosis,[16] and hepatic ischemia reperfusion injury.[17]

With regard to genotoxicity, HNE induces an SOS response in *Escherichia coli*.[18] Chromosomal aberrations are observed

(1) Benedetti, A.; Comporti, M.; Esterbauer, H. *Biochim. Biophys. Acta* **1980**, *620*, 281–296.
(2) Esterbauer, H.; Schaur, R. J.; Zollner, H. *Free Radical Biol. Med.* **1991**, *11*, 81–128.
(3) Burcham, P. C. *Mutagenesis* **1998**, *13*, 287–305.
(4) Lee, S. H.; Blair, I. A. *Chem. Res. Toxicol.* **2000**, *13*, 698–702.
(5) Schneider, C.; Tallman, K. A.; Porter, N. A.; Brash, A. R. *J. Biol. Chem.* **2001**, *276*, 20831–20838.
(6) Schneider, C.; Porter, N. A.; Brash, A. R. *J. Biol. Chem.* **2008**, *283*, 15539–15543.
(7) Parola, M.; Bellomo, G.; Robino, G.; Barrera, G.; Dianzani, M. U. *Antioxid. Redox Signaling* **1999**, *1*, 255–284.
(8) Poli, G.; Schaur, R. J. *IUBMB Life* **2000**, *50*, 315–321.
(9) Nakashima, I.; Liu, W.; Akhand, A. A.; Takeda, K.; Kawamoto, Y.; Kato, M.; Suzuki, H. *Mol. Aspects Med.* **2003**, *24*, 231–238.
(10) West, J. D.; Ji, C.; Duncan, S. T.; Amarnath, V.; Schneider, C.; Rizzo, C. J.; Brash, A. R.; Marnett, L. J. *Chem. Res. Toxicol.* **2004**, *17*, 453–462.
(11) West, J. D.; Marnett, L. J. *Chem. Res. Toxicol.* **2005**, *18*, 1642–1653.
(12) West, J. D.; Marnett, L. J. *Chem. Res. Toxicol.* **2006**, *19*, 173–194.
(13) Dwivedi, S.; Sharma, A.; Patrick, B.; Sharma, R.; Awasthi, Y. C. *Redox Rep.* **2007**, *12*, 4–10.
(14) Sayre, L. M.; Zelasko, D. A.; Harris, P. L.; Perry, G.; Salomon, R. G.; Smith, M. A. *J. Neurochem.* **1997**, *68*, 2092–2097.
(15) Yoritaka, A.; Hattori, N.; Uchida, K.; Tanaka, M.; Stadtman, E. R.; Mizuno, Y. *Proc. Natl. Acad. Sci. U.S.A.* **1996**, *93*, 2696–2701.
(16) Napoli, C.; D'Armiento, F. P.; Mancini, F. P.; Postiglione, A.; Witztum, J. L.; Palumbo, G.; Palinski, W. *J. Clin. Invest.* **1997**, *100*, 2680–2690.
(17) Yamagami, K.; Yamamoto, Y.; Kume, M.; Ishikawa, Y.; Yamaoka, Y.; Hiai, H.; Toyokuni, S. *Antioxid. Redox Signaling* **2000**, *2*, 127–136.
(18) Benamira, M.; Marnett, L. J. *Mutat. Res.* **1992**, *293*, 1–10.

10.1021/ja801824b CCC: $40.75

Chart 1. Formation of Exocyclic 1,N^2-dG Adducts **2**-**5** by HNE

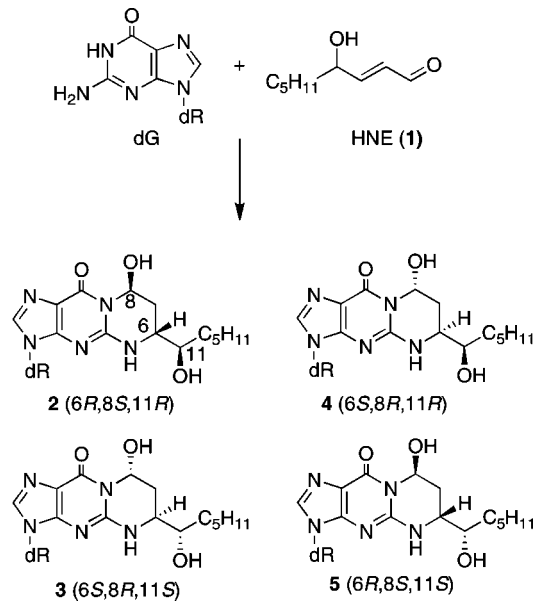

upon exposure to HNE in rodent,[19,20] mammalian,[21,22] and human[23] cells. In mammalian cells, the genotoxicity of HNE depends upon glutathione levels, which modulate the formation of HNE-DNA adducts.[24–26] Michael addition of the N^2-amino group of deoxyguanosine to HNE gives four diastereomeric exocyclic 1,N^2-dG adducts **2**−**5** (Chart 1),[27–29] which have been detected in cellular DNAs.[30–36] Alternatively, oxidation of HNE to 2,3-epoxy-4-hydroxynonanal, and further reaction with nucleobases, affords substituted etheno adducts.[37–41]

Chart 2. Nucleotide Numbering Scheme of the Dodecamer Containing the 5′-C⁶pX⁷-3′ Sequence Context; X Represents the Position of the HNE-Derived Exocyclic 1,N^2-dG Adducts **2** or **3**

5′-G¹ C² T³ A⁴ G⁵ C⁶ **X**⁷ A⁸ G⁹ T¹⁰C¹¹C¹²-3′
3′-C²⁴G²³A²²T²¹C²⁰G¹⁹C¹⁸T¹⁷C¹⁶A¹⁵G¹⁴G¹³-5′

X⁷ = **2** or **3**

The mutational spectrum induced by HNE in the *lacZ* gene of the single-stranded M13 phage transfected into wild-type *E. coli* revealed recombination events, C → T transitions, followed by G → C and A → C transversions, and frameshift mutations.[29] HNE is mutagenic[42] and carcinogenic in rodent cells.[43] Hussain et al.[44] reported that HNE caused G·C → T·A transversions at codon 249 of wild-type *p53* in lymphosblastoid cells. Hu et al.[45] further reported that HNE-DNA adducts were preferentially formed with guanine at the third base of codon 249 in the *p53* gene. The mutational spectrum induced by *trans*-4-hydroxynonenal-derived deoxyguanosine (HNE-dG) adducts in the *supF* gene of shuttle vector pSP189 replicated in human cells showed that HNE induced primarily G → T transversions, accompanied by lower levels of G → A transitions.[46] Fernandes et al.[47] conducted site-specific mutagenesis studies and observed that, in the 5′-CpG-3′ duplex of interest in the present work, only stereoisomers **2** and **3** of the HNE-induced exocyclic 1,N^2-dG adduct were mutagenic, inducing low levels of G → T transversions and G → A transitions. Evidence has been obtained that nucleotide excision repair pathway is involved in the repair of HNE-dG lesion.[46,48,49]

Wang et al.[50,51] synthesized the four stereoisomers of the HNE-derived exocyclic 1,N^2-dG Michael addition products (**2**−**5**) and incorporated them into 5′-d(GCTAGCXAGTCC)-3′·5′-d(GGACTCGCTAGC)-3′, in which X denotes the HNE-dG adduct (Chart 2). The related deoxyguanosine adducts of acrolein[52–55] and crotonaldehyde[56] formed interchain cross-links

(19) Esterbauer, H.; Eckl, P.; Ortner, A. *Mutat. Res.* **1990**, *238*, 223–233.
(20) Eckl, P. M.; Ortner, A.; Esterbauer, H. *Mutat. Res.* **1993**, *290*, 183–192.
(21) Karlhuber, G. M.; Bauer, H. C.; Eckl, P. M. *Mutat. Res.* **1997**, *381*, 209–216.
(22) Eckl, P. M. *Mol. Aspects Med.* **2003**, *24*, 161–165.
(23) Emerit, I.; Khan, S. H.; Esterbauer, H. *Free Radical Biol. Med.* **1991**, *10*, 371–377.
(24) Chung, F. L.; Komninou, D.; Zhang, L.; Nath, R.; Pan, J.; Amin, S.; Richie, J. *Chem. Res. Toxicol.* **2005**, *18*, 24–27.
(25) Falletti, O.; Cadet, J.; Favier, A.; Douki, T. *Free Radical Biol. Med.* **2007**, *42*, 1258–1269.
(26) Yadav, U. C.; Ramana, K. V.; Awasthi, Y. C.; Srivastava, S. K. *Toxicol. Appl. Pharmacol.* **2008**, *227*, 257–264.
(27) Winter, C. K.; Segall, H. J.; Haddon, W. F. *Cancer Res.* **1986**, *46*, 5682–5686.
(28) Douki, T.; Odin, F.; Caillat, S.; Favier, A.; Cadet, J. *Free Radical Biol. Med.* **2004**, *37*, 62–70.
(29) Kowalczyk, P.; Ciesla, J. M.; Komisarski, M.; Kusmierek, J. T.; Tudek, B. *Mutat. Res.* **2004**, *550*, 33–48.
(30) Yi, P.; Zhan, D.; Samokyszyn, V. M.; Doerge, D. R.; Fu, P. P. *Chem. Res. Toxicol.* **1997**, *10*, 1259–1265.
(31) Chung, F. L.; Nath, R. G.; Ocando, J.; Nishikawa, A.; Zhang, L. *Cancer Res.* **2000**, *60*, 1507–1511.
(32) Wacker, M.; Schuler, D.; Wanek, P.; Eder, E. *Chem. Res. Toxicol.* **2000**, *13*, 1165–1173.
(33) Wacker, M.; Wanek, P.; Eder, E. *Chem.-Biol. Interact.* **2001**, *137*, 269–283.
(34) Chung, F. L.; Zhang, L. *Methods Enzymol.* **2002**, *353*, 523–536.
(35) Liu, X.; Lovell, M. A.; Lynn, B. C. *Chem. Res. Toxicol.* **2006**, *19*, 710–718.
(36) Pan, J.; Davis, W.; Trushin, N.; Amin, S.; Nath, R. G.; Salem, N., Jr.; Chung, F. L. *Anal. Biochem.* **2006**, *348*, 15–23.
(37) Sodum, R. S.; Chung, F. L. *Cancer Res.* **1988**, *48*, 320–323.
(38) Sodum, R. S.; Chung, F. L. *Chem. Res. Toxicol.* **1989**, *2*, 23–28.
(39) Sodum, R. S.; Chung, F. L. *Cancer Res.* **1991**, *51*, 137–143.
(40) Chen, H. J.; Chung, F. L. *Chem. Res. Toxicol.* **1994**, *7*, 857–860.
(41) el Ghissassi, F.; Barbin, A.; Nair, J.; Bartsch, H. *Chem. Res. Toxicol.* **1995**, *8*, 278–283.
(42) Cajelli, E.; Ferraris, A.; Brambilla, G. *Mutat. Res.* **1987**, *190*, 169–171.
(43) Chung, F. L.; Chen, H. J.; Guttenplan, J. B.; Nishikawa, A.; Hard, G. C. *Carcinogenesis* **1993**, *14*, 2073–2077.
(44) Hussain, S. P.; Raja, K.; Amstad, P. A.; Sawyer, M.; Trudel, L. J.; Wogan, G. N.; Hofseth, L. J.; Shields, P. G.; Billiar, T. R.; Trautwein, C.; Hohler, T.; Galle, P. R.; Phillips, D. H.; Markin, R.; Marrogi, A. J.; Harris, C. C. *Proc. Natl. Acad. Sci. U.S.A.* **2000**, *97*, 12770–12775.
(45) Hu, W.; Feng, Z.; Eveleigh, J.; Iyer, G.; Pan, J.; Amin, S.; Chung, F. L.; Tang, M. S. *Carcinogenesis* **2002**, *23*, 1781–1789.
(46) Feng, Z.; Hu, W.; Amin, S.; Tang, M. S. *Biochemistry* **2003**, *42*, 7848–7854.
(47) Fernandes, P. H.; Wang, H.; Rizzo, C. J.; Lloyd, R. S. *Environ. Mol. Mutagen.* **2003**, *42*, 68–74.
(48) Chung, F. L.; Pan, J.; Choudhury, S.; Roy, R.; Hu, W.; Tang, M. S. *Mutat. Res.* **2003**, *531*, 25–36.
(49) Choudhury, S.; Pan, J.; Amin, S.; Chung, F. L.; Roy, R. *Biochemistry* **2004**, *43*, 7514–7521.
(50) Wang, H.; Rizzo, C. J. *Org. Lett.* **2001**, *3*, 3603–3605.
(51) Wang, H.; Kozekov, I. D.; Harris, T. M.; Rizzo, C. J. *J. Am. Chem. Soc.* **2003**, *125*, 5687–5700.
(52) Kozekov, I. D.; Nechev, L. V.; Sanchez, A.; Harris, C. M.; Lloyd, R. S.; Harris, T. M. *Chem. Res. Toxicol.* **2001**, *14*, 1482–1485.
(53) Kozekov, I. D.; Nechev, L. V.; Moseley, M. S.; Harris, C. M.; Rizzo, C. J.; Stone, M. P.; Harris, T. M. *J. Am. Chem. Soc.* **2003**, *125*, 50–61.
(54) Kim, H. Y.; Voehler, M.; Harris, T. M.; Stone, M. P. *J. Am. Chem. Soc.* **2002**, *124*, 9324–9325.
(55) Cho, Y. J.; Kim, H. Y.; Huang, H.; Slutsky, A.; Minko, I. G.; Wang, H.; Nechev, L. V.; Kozekov, I. D.; Kozekova, A.; Tamura, P.; Jacob, J.; Voehler, M.; Harris, T. M.; Lloyd, R. S.; Rizzo, C. J.; Stone, M. P. *J. Am. Chem. Soc.* **2005**, *127*, 17686–17696.
(56) Cho, Y. J.; Wang, H.; Kozekov, I. D.; Kurtz, A. J.; Jacob, J.; Voehler, M.; Smith, J.; Harris, T. M.; Lloyd, R. S.; Rizzo, C. J.; Stone, M. P. *Chem. Res. Toxicol.* **2006**, *19*, 195–208.

Chart 3. Ring-Opening Chemistry of the HNE-Derived Exocyclic 1,N^2-dG Adducts **2** and **3** When Placed opposite dC in Duplex DNA

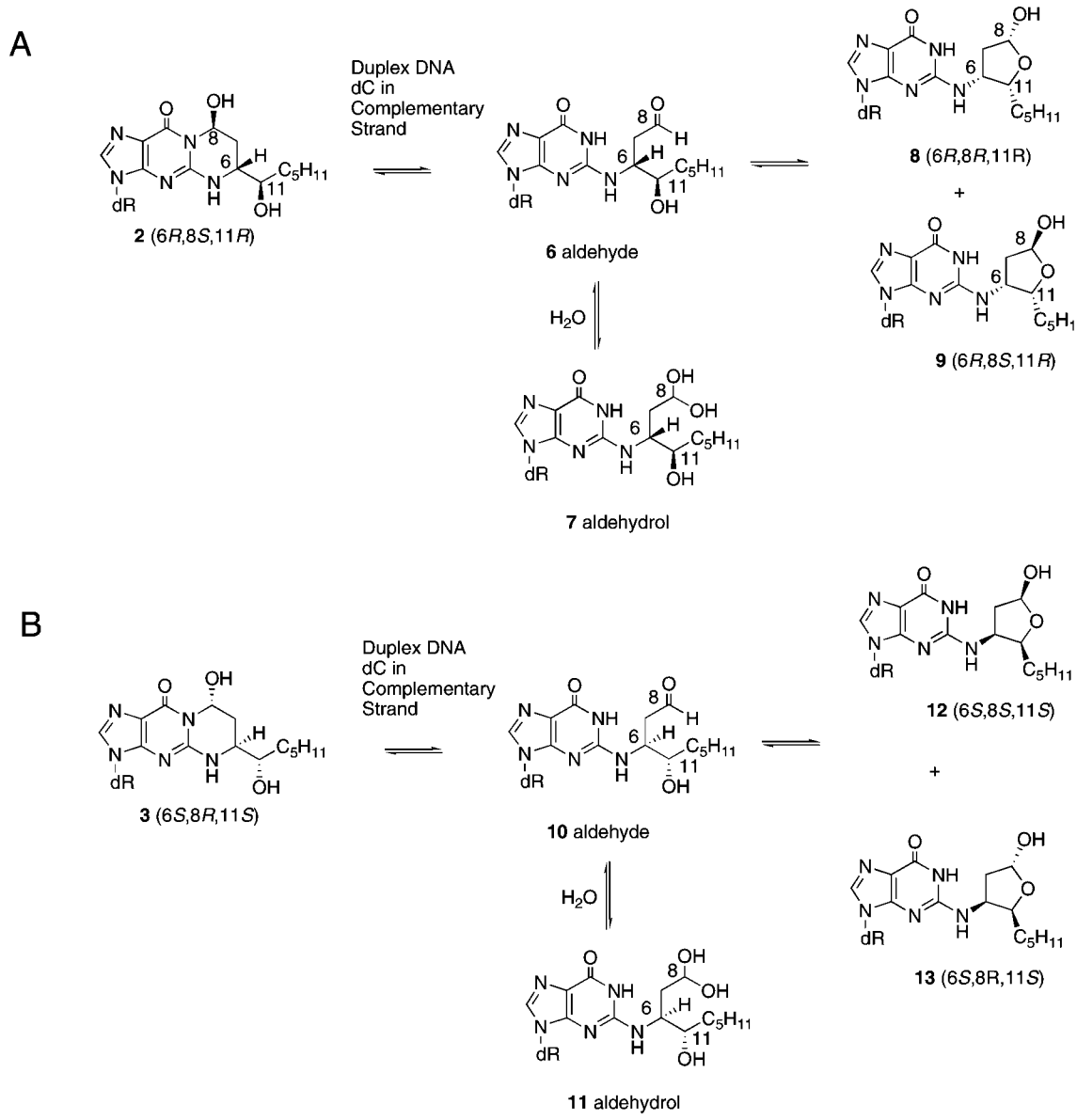

in this 5′-CpG-3′ sequence context.[57] In the case of the crotonaldehyde adduct, the 6*R* stereoisomer formed cross-links more efficiently than did the 6*S* stereoisomer.[53] Of the four HNE-dG adducts (**2**−**5**), only stereoisomer **3** possessing (6*S*,8*R*,11*S*) stereochemistry resulted in DNA interchain cross-link formation.[51] Significantly, this HNE isomer possessed the same relative stereochemistry as the 6*R* crotonaldehyde adduct. However, cross-link formation was slow.[51] Kurtz and Lloyd[58] demonstrated that HNE adduct **3** formed a conjugate with the tetrapeptide KWKK more rapidly than did the other three stereoisomeric HNE adducts **2**, **4**, and **5**.

In the present work, we demonstrate that, similar to the related exocyclic 1,N^2-dG adducts of acrolein[59] and crotonaldehyde,[56] when placed opposite cytosine in the dodecamer containing the 5′-C^{6}pX^7-3′ sequence context (Chart 2), the diastereomeric HNE-dG adducts **2** and **3** (Chart 1) undergo ring-opening to aldehydes **6** and **10** (Chart 3); the ring-opened aldehydes exist in equilibrium with hydrated aldehydrols **7** and **11** (Chart 3). In contrast to the acrolein[59] and crotonaldehyde[56] adducts, the presence of the γ-hydroxyl group in aldehydes **6** and **10** allows for further rearrangments to cyclic hemiacetals **8** and **9**, and **12** and **13**, respectively (Chart 3), as have been observed for the Michael addition of protein nucleophiles to HNE.[60]

Results

Watson−Crick Base Pairing of DNA Duplex Containing (6*R*,8*S*,11*R*) Adduct 2. Figure 1A shows the NOE connectivity of the purine N1 and pyrimidine N3 imino protons. An imino proton resonance was observed for the modified purine X^7. This suggested that, when placed opposite dC in this DNA duplex,

(57) Stone, M. P.; Cho, Y.-J.; Huang, H.; Kim, H.-Y.; Kozekov, I. D.; Kozekova, A.; Wang, H.; Minko, I. G.; Lloyd, R. S.; Harris, T. M.; Rizzo, C. J. Acc. Chem. Res. [Online early access]. DOI: 10.1021/ar700246x. Published Online: May 24, 2008. http://pubs.acs.org/cgi-bin/abstract.cgi/achre4/asap/abs/ar700246x.html.

(58) Kurtz, A. J.; Lloyd, R. S. *J. Biol. Chem.* **2003**, *278*, 5970–5976.

(59) de los Santos, C.; Zaliznyak, T.; Johnson, F. *J. Biol. Chem.* **2001**, *276*, 9077–9082.

(60) Sayre, L. M.; Lin, D.; Yuan, Q.; Zhu, X.; Tang, X. *Drug Metab. Rev.* **2006**, *38*, 651–675.

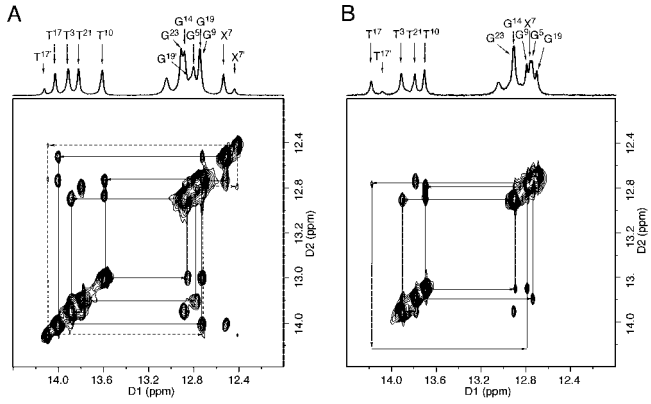

Figure 1. (A) ^{1}H NOESY spectra (250 ms) of the HNE-modified duplex containing stereoisomer **2** showing the sequential connectivity of the imino protons involved in hydrogen bonding. Solid lines represent the sequential connectivity pattern of the major species. Dashed lines are assigned to a minor species involving the X^7, T^{17}, and G^{19} imino protons. (B) ^{1}H NOESY spectra (250 ms) of the HNE-modified duplex containing stereoisomer **3** showing the sequential connectivity of the imino protons involved in hydrogen bonding. Solid lines represent the sequential connectivity pattern of the major species. The broad resonance at 14.0 ppm is assigned to the T^{17} imino proton of the minor species.

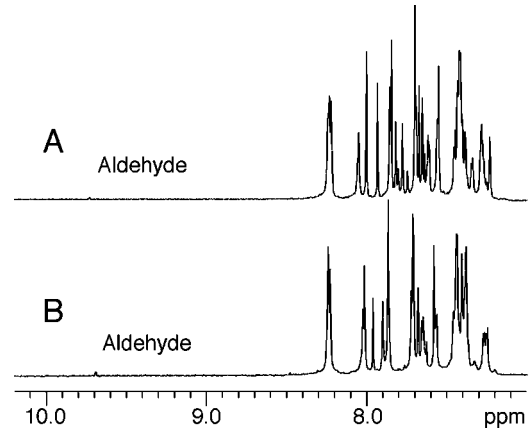

Figure 2. (A) ^{1}H NMR of the DNA duplex containing stereoisomer **2**, showing the aldehyde resonance at ~9.7 ppm. (B) ^{1}H NMR of the DNA duplex bearing stereoisomer **3**, showing the aldehyde resonance at ~9.7 ppm.

exocyclic 1,N^2-dG adduct **2** had undergone ring-opening, presumably to aldehyde **6**.[59] Consequently, a complete NOE connectivity was obtained for the purine N1 and pyrimidine N3 imino protons of the duplex.[61] A strong NOE was observed between X^7 N9H → X^7 N5H (the X^7 amino and imino protons are designated N5H and N9H, respectively), suggesting that the exocyclic amino group X^7 N5H was sheltered from exchange with solvent. A second NOE connectivity involving the X^7, T^{17}, and G^{19} imino protons was observed. These resonances were assigned to a minor species. Similar to the major species, the imino resonance X^7 N9H of the minor species exhibited a cross-peak with X^7 N5H.

Nature of the HNE-Modified Nucleotide 2. As noted, observation of imino resonances corresponding to major and minor species involving the modified purine X^7 suggested that adduct **2** had undergone ring-opening to aldehyde **6** when placed opposite dC in this DNA duplex (Chart 3).[59] An expansion of the ^{1}H NMR spectrum is shown in Figure 2A. The weak resonance observed at 9.7 ppm confirmed the presence of the anticipated aldehyde. However, the aldehyde signal did not integrate proportionally with the oligodeoxynucleotide protons (Figure 2), suggesting that it was present at only trace levels and existed in equilibrium with another species.

The possibility that, upon ring-opening of adduct **2**, the resulting aldehyde **6** had further converted to aldehydrol **7** was considered (Chart 3). Aldehydes equilibrate with the corresponding aldehydrols in aqueous solution, which has been observed for the ring-opened 1,N^2-dG adducts of acrolein and crotonaldehyde.[55,56,59] MALDI-TOF mass spectrometric analysis yielded a molecular weight for the adducted strand of 3801.9 Da, which was inconsistent with aldehydrol **7**. The possibility that the γ-hydroxyl group could cyclize with the aldehyde in the ring-opened HNE adduct, to afford stereoisomeric cyclic hemiacetals **8** and **9**, was considered (Chart 3).[62,63] Related cyclic hemiacetals of cysteine, histidine, and lysine Michael addition products of HNE were characterized.[60] The calculated mass of the cyclic hemiacetal form of 3800.8 Da (M − H) was in agreement with the observed mass spectrometric analysis of 3801.8 Da. Aldehyde **6**, cyclic hemiacetals **8** and **9**, and exocyclic 1,N^2-dG adduct **2** share the same mass. However, the NMR data (*vide infra*) were not consistent with the significant presence of exocyclic 1,N^2-dG adduct **2** or aldehyde **6**. The existence of γ-hydroxyl group in aldehyde **6** was anticipated to facilitate formation of cyclic hemiacetals **8** and **9**. The formation of cyclic hemiacetals was not anticipated to be highly stereoselective. For example, the HNE−histidine conjugate weakly preferred the *trans* configuration of the aliphatic chain with the hydroxyl group.[62] Thus, in agreement with the mass spectrometric data, the two sets of NMR resonances observed for the HNE protons were attributed to the formation of diastereomeric hemiacetals **8** and **9**, and not diol **7**, the latter which could exist only in a single configuration. The chemical shifts of the HNE H6 and H11 protons (Table 1) were also consistent with those observed for the cyclic hemiacetal HNE−histidine conjugates.[62]

In the double-quantum filtered correlation spectroscopy (DQF-COSY) spectrum, a resonance observed at 5.45 ppm exhibited both dipolar and scalar couplings to a resonance observed at 2.13 ppm (Figure 3A). This was assigned as a correlation between X^7 H8 and the vicinal X^7 H7$^\beta$ proton. Another resonance, observed at 3.93 ppm, exhibited scalar coupling to a resonance observed at 2.15 ppm (Figure 3A) and was assigned as a correlation between X^7 H6 and the X^7 H7$^\alpha$ proton. These assignments were corroborated by nuclear Overhauser effect spectroscopy (NOESY) data obtained at a mixing time of 60 ms. The difference of the chemical shifts of the two geminal X^7 H7 protons was <0.02 ppm. Both X^7 H7 protons exhibited NOE cross-peaks with X^7 H6 and X^7 H8. The correlations X^7 H6 → X^7 H11 and X^7 H11 → X^7 H12(s), observed in both NOESY and DQF-COSY spectra, were used to assign the resonances of the X^7 H11 and X^7 H12 protons. The resonances of X^7 H12−H16 were overlapped. The X^7 H6−H8, H11, and H12 resonances of the minor species were similarly assigned from DQF-COSY and NOESY spectra. Because of overlap, the X^7 H13−H16 resonances of the minor species were not assigned. The ^{1}H NMR spectra of the major and the minor species were similar, although the geminal X^7

(61) Boelens, R.; Scheek, R. M.; Dijkstra, K.; Kaptein, R. *J. Magn. Reson.* **1985**, *62*, 378–386.
(62) Hashimoto, M.; Sibata, T.; Wasada, H.; Toyokuni, S.; Uchida, K. *J. Biol. Chem.* **2003**, *278*, 5044–5051.
(63) Beretta, G.; Artali, R.; Regazzoni, L.; Panigati, M.; Facina, R. M. *Chem. Res. Toxicol.* **2007**, *20*, 1309–1314.

Table 1. ^{1}H Chemical Shifts of the Cyclic Hemiacetal Adducts **8** and **9** and **12** and **13**, Derived from Exocyclic 1,N^2-dG Adducts **2** and **3**, When Placed opposite dC in Duplex DNA

1,N^2-dG adduct		**2** (6*R*,8*S*,11*R*)		**3** (6*S*,8*R*,11*S*)	
cyclic hemiacetal		**8** (6*R*,8*R*,11*R*) minor	**9** (6*R*,8*S*,11*R*) major	**12** (6*S*,8*S*,11*S*) minor	**13** (6*S*,8*R*,11*S*) major
chemical shift (ppm)	H6	3.85	3.93	4.15	4.55
	H7$^\alpha$	1.80	2.13	1.75	2.17
	H7$^\beta$	2.59	2.15	2.64	2.17
	H8	5.28	5.45	5.33	5.43
	H11	3.96	4.26	4.05	4.23
	H12$^\alpha$	1.45	1.33	1.39	1.34
	H12$^\beta$	1.56	1.41	1.53	1.45
	H13		1.27		1.36
	H14		1.15		1.45
	H15		1.20		1.38
	H16		0.82		0.96

H7 protons of the minor species exhibited greater chemical shift resolution. The chemical shift assignments are summarized in Table 1.

It was concluded that the major and minor species of the ring-opened HNE-dG adducts were stereoisomeric cyclic hemiacetals **8** and **9** (Chart 3). The major species showed a strong H8 → H7$^\beta$ NOE correlation and a weaker H8 → H7$^\alpha$ NOE, whereas the H6 → H7$^\alpha$ NOE was stronger than the H6 → H7$^\beta$ NOE, suggesting that X^7 H6 and X^{7}H8 were in the trans configuration. That is, cyclic stereoisomer **9** (6*R*,8*S*,11*R*) was the major species at equilibrium and stereoisomer **8** (6*R*,8*R*,11*R*) was the minor species. Modeling studies of the DNA duplex showed that the (6*R*,8*S*,11*R*) configuration agreed with the X^7 H8 → C^{18} H1′, X^7 H8 → G^{19} H1′, and X^7 H8 → G^{19} H4′ NOEs observed for the major species.

Other Nucleotides of the Duplex Containing Stereoisomer 2. Figure 4 shows an expansion of the ^{1}H NOESY spectrum. The nonexchangeable protons of nucleosides were assigned on

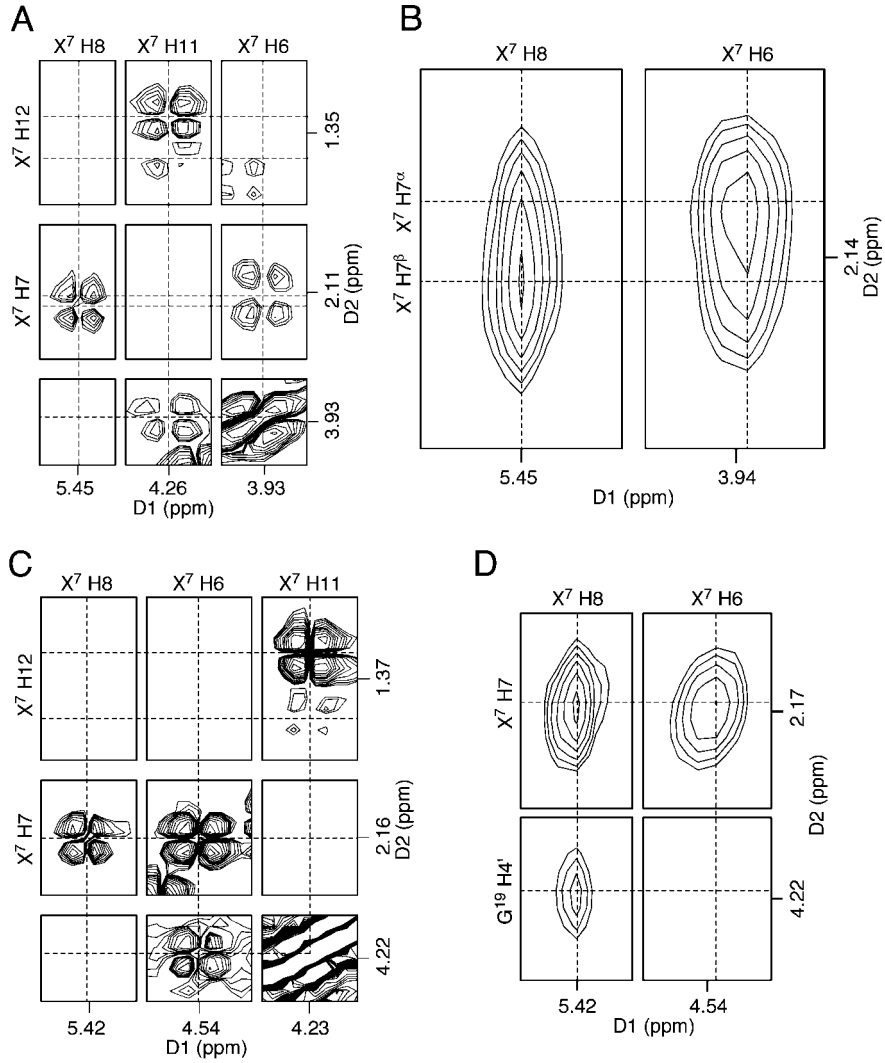

Figure 3. DQF-COSY and NOESY correlations used to assign resonances of X^7 H6−H12 protons of the major species derived from stereoisomer **2**: (A) DQF-COSY and (B) NOESY (60 ms). DQF-COSY and NOESY correlations used to assign resonances of X^7 H6−H12 protons of the major species derived from stereoisomer **3**: (C) DQF-COSY and (D) NOESY (60 ms).

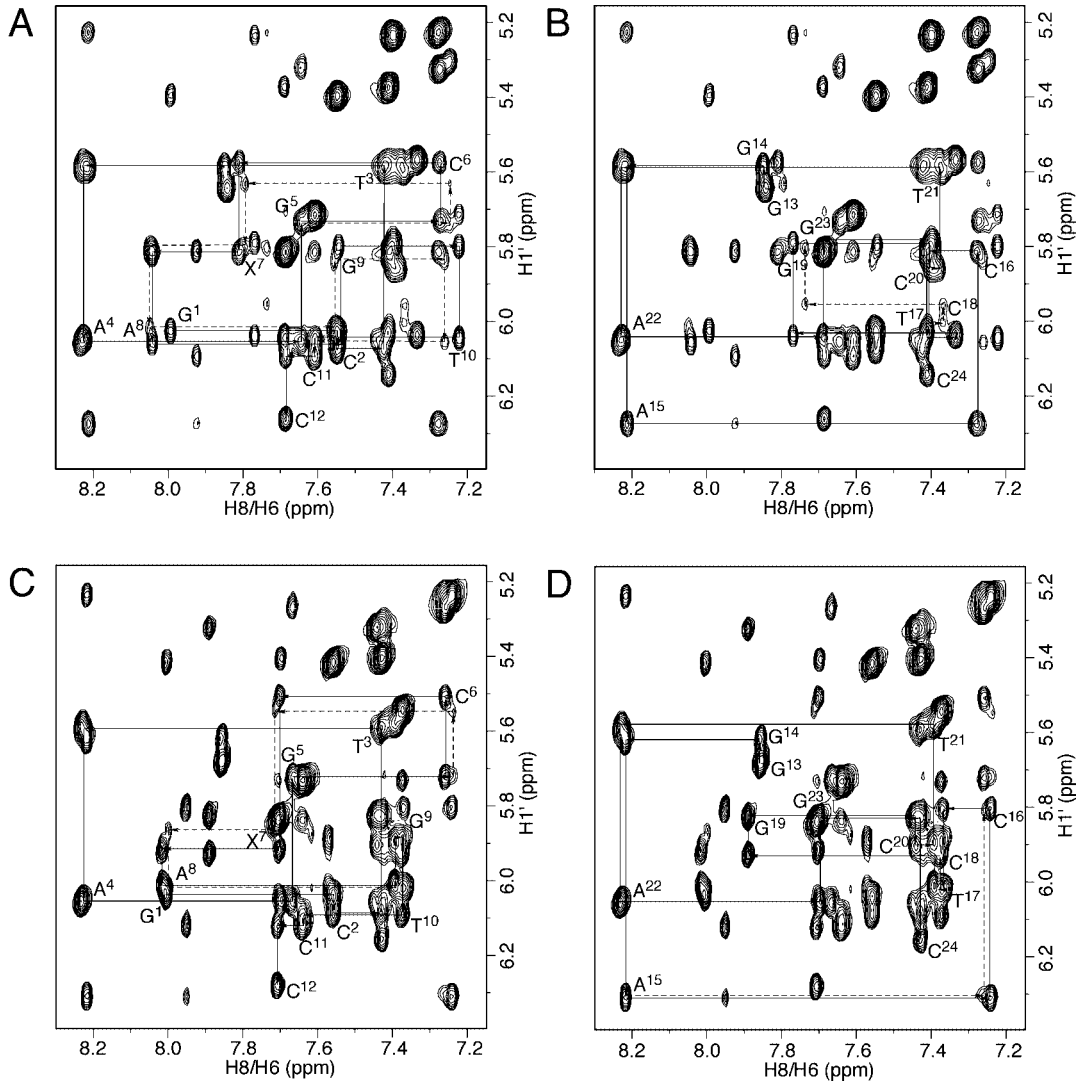

Figure 4. NOESY spectra (250 ms) of the HNE-modified duplexes containing stereoisomers **2** and **3**, showing the correlations of aromatic H6 and H8 protons with deoxyribose H1′ protons. (A) Modified strand containing stereoisomer **2**. (B) Complementary strand containing stereoisomer **2**. (C) Modified strand containing stereoisomer **3**. (D) Complementary strand containing stereoisomer **3**. Solid lines indicate the major species; dotted lines represent the minor species.

the basis of the sequential connectivity of the base proton H6 or H8 (the base proton of X^7 is designated as H2) dipolar couplings with H1′ sugar protons.[64,65] A complete sequential connectivity was observed for both the modified and the complementary strand of the major species (Figure 4A,B solid lines). A sequential connectivity was also observed for the minor species (Figure 4A,B dashed lines). In the modified strand, these extended from $G^5 \rightarrow C^6 \rightarrow X^7 \rightarrow A^8 \rightarrow G^9 \rightarrow T^{10} \rightarrow C^{11}$. Most nucleoside protons of the major species as well as some protons of the minor species were assigned.

Watson−Crick Base Pairing of DNA Duplex Containing the (6*S*,8*R*,11*S*) Adduct 3. Figure 1B shows the imino region of the NOESY spectrum. Sequential NOEs including the adducted guanine X^7 were observed, indicating that the adduct had undergone ring-opening. The T^{17} N3H resonance was broad, and the diagonal peak in the NOESY spectrum was missing, suggesting that base pair $A^8 \cdot T^{17}$ was perturbed by the incorporation of stereoisomer **3**. This may contribute to the observed 4 °C lower thermal stability (T_m) of the DNA duplex containing stereoisomer **3** as compared to the duplex containing stereoisomer **2**.[51] However, weak T^{17} N3H → X^7 N9H, T^{17} N3H → G^9 N1H, and T^{17} N3H → A^8 H2 NOEs were observed. This suggested that the $A^8 \cdot T^{17}$ base pair adopted a weak Watson−Crick hydrogen bonding. Similar to the duplex containing stereoisomer **2**, the imino proton X^7 N9H exhibited a strong NOE to the amino proton X^7 N5H. A small peak was observed at 14.0 ppm and assigned as the T^{17} imino proton of a minor species; this signal was broad and weak when compared to the duplex of stereoisomer **2**. The anticipated imino proton resonances for X^7 and G^{19} of the minor species could not be assigned because of overlapping resonances and line broadening.

Nature of the HNE-Modified Nucleotide 3. Figure 2B shows an expansion of the ^{1}H NMR spectrum of the HNE-modified duplex. A weak peak was observed at ∼9.7 ppm and assigned as an aldehyde. It did not integrate proportionally with the oligodeoxynucleotide protons, suggesting that the aldehyde was present in trace amounts. Mass spectrometric analysis gave a molecular mass of 3803.8 Da, in agreement with the formation of cyclic hemiacetals (calcd for M − H, 3800.8 Da), as opposed

(64) Reid, B. R. *Q. Rev. Biophys.* **1987**, *20*, 2–28.
(65) Patel, D. J.; Shapiro, L.; Hare, D. *Q. Rev. Biophys.* **1987**, *20*, 35–112.

to the aldehydrol (calcd for M − H, 3818.8 Da). As was observed for the duplex containing stereoisomer **2**, two sets of NMR resonances were observed for the HNE protons, consistent with the formation of diastereomeric hemiacetals **12** and **13** (Chart 3). The chemical shifts of the H6 and H11 HNE proton resonances were consistent with the reported chemical shifts of cyclic hemiacetal HNE−histidine conjugates.[62]

The assignment of HNE protons followed the same strategy as that for the duplex containing stereoisomer **2** (Table 1). Of note, the geminal H7 protons of the major species were not resolved (Figure 3C,D) for **3**. NOESY spectra revealed that X^7 H8 strongly correlated with G^{19} H4′. A strong NOE cross-peak was observed at 60-ms mixing time (Figure 3D), indicating that X^7 H8 and G^{19} H4′ were proximate. Modeling studies indicated that the R configuration of X^7 C8 placed X^7 H8 2.4−3.6 Å from G^{19} H4′. In contrast, the S configuration of X^7 C8 placed X^7 H8 4.0−5.1 Å from G^{19} H4′. Therefore, the strong X^7 H8 → G^{19} H4′ NOE suggested that cyclic hemiacetal stereoisomer **13** (6*S*,8*R*,11*S*) was the major species derived from the ring-opening of HNE adduct **3**, and consequently, stereoisomer **12** (6*S*,8*S*,11*S*) was the minor species (Chart 3). Modeling studies of the DNA duplex also showed that the (6*S*,8*R*,11*S*) configuration agreed well with X^7 H8 → C^{18} H1′, X^7 H8 → G^{19} H1′, X^7 H8 → G^{19} H5′, and X^7 H8 → G^{19} H5″ correlations. Some HNE resonances of the minor species were assigned on the basis of DQF-COSY and NOESY spectra. In contrast to the major species, the geminal X^7 H7 protons of the minor species were resolved. Because of overlap, the X^7 H13−H16 resonances of the minor species were not assigned (Table 1). Except for X^7 H6, all HNE protons of the major species derived from stereoisomers **2** and **3** had similar chemical shifts, indicating similar structures. The X^7 H6 protons derived from stereoisomers **2** and **3** exhibited a chemical shift difference of 0.62 ppm, indicating different chemical environments of the X^7 H6 protons for these stereoisomers.

Other Nucleotides of the Duplex Containing Stereoisomer 3. Figure 4C,D shows an expansion of the ^{1}H NOESY spectrum. The nonexchangeable protons of the nucleotides were assigned on the basis of the sequential connectivity of the base proton H6 or H8 (the base proton of X^7 is designated as H2) dipolar couplings with H1′ sugar protons.[64,65] A complete sequential connectivity was observed for both the modified and the complementary strand (Figure 4C,D solid lines). A second sequential connectivity was observed (Figure 4C,D dashed lines). In the modified strand, these extended from C^6 → X^7 → A^8. These were assigned to the minor species.

Discussion

The Michael addition of HNE to deoxyguanosine in DNA gives four diastereomeric exocyclic 1,N^2-deoxyguanosine adducts (**2**−**5**) (Chart 1).[27–29,57] Incorporation of the exocyclic 1,N^2-dG structure into duplex DNA precludes Watson−Crick hydrogen bonding and results in structural[66–69] and thermodynamic[70] perturbations at the lesion and complementary nucleotides. On the basis of observations with the corresponding exocyclic 1,N^2-dG adducts arising from acrolein[59] and crotonaldehyde[56] in DNA, it was anticipated that the adducts **2**−**5** (Chart 1) would undergo ring-opening to aldehydes when placed opposite cytosine in duplex DNA. The resulting aldehydes might then form interstrand cross-links in the 5′-CpG-3′ sequence.[52–57] Significantly, when HNE adducts **2**−**5** were incorporated into the dodecamer containing the 5′-CpX-3′ sequence (Chart 2) and examined as to their respective abilities to form interstrand cross-links, only stereoisomer **3** formed interstrand cross-links.[51] Consequently, it was of interest to examine in greater detail the structure of the non-cross-linking stereoisomer **2** vs that of the cross-linking stereoisomer **3** when placed into duplex DNA opposite cytosine. The specific comparison of stereoisomers **2** vs **3** was also relevant because they possessed the same relative stereochemistry at C6 as did the corresponding 6*R* and 6*S* stereoisomers of the crotonaldehyde adduct, of which the 6*R* adduct formed interstrand cross-links much more efficiently[53] (note that the R vs S designation at C6 is reversed for the HNE adducts as compared to that of the crotonaldehyde adducts).[51] Moreover, both HNE stereoisomers induced low levels of G → T mutations in the mammalian COS-7 cell assay, whereas stereoisomers **4** and **5** were largely inactive in the site-specific mutagenesis studies.[47]

HNE-Derived Exocyclic 1,N^2-dG Adducts 2 and 3 Rearrange to Diastereomeric N^2-dG Cyclic Hemiacetal Adducts When Placed opposite Cytosine in Duplex DNA. The HNE-derived 1,N^2-dG adducts **2** and **3** bear exocyclic rings through the bonding of guanine N1 and N^2 to the HNE moiety; Watson−Crick hydrogen bonding is not possible. The NMR data indicate that when either exocyclic adduct **2** or **3** was placed into duplex DNA opposite cytosine, ring-opening to aldehydes **6** and **10** occurred (Chart 3, Figures 1 and 2). Riggins et al.[71,72] reported mechanistic studies of the ring-opening and -closing of the structurally related malondialdehyde-derived adduct 3-(2′-deoxy-β-D-erythropentofuranosyl)pyrimido[1,2-α]purin-10(3*H*)-one (M_1dG). They concluded that ring-opening of M_1dG as a nucleoside or in oligodeoxynucleotides occurred via a reversible second-order reaction with hydroxide ion and was catalyzed by the complementary cytosine in duplex DNA. The closure of the resulting N^2-(3-oxo-1-propenyl)deoxyguanosine anion was pH-dependent, and under neutral and acidic conditions ring closure was biphasic, leading to the rapid formation of intermediates that slowly converted to M_1dG in a general-acid-catalyzed reaction.

In contrast to the corresponding acrolein[59] and crotonaldehyde[56] adducts, the major forms of the ring-opened species arising from HNE adducts **2** or **3** were not the aldehydes **6** and **10** when at equilibrium in duplex DNA (Chart 3). Only trace amounts of aldehydes **6** and **10** were derived from the ring-opening of exocyclic 1,N^2-dG adducts **2** and **3**. For the exocyclic 1,N^2-dG adducts derived from acrolein[59] and crotonaldehyde[56] in an identical sequence, the ring-opened aldehydes were observed to be in equilibrium with the corresponding aldehydrols. However, our spectroscopic data indicate that cyclic hemiacetals **8** and **9**, or **12** and **13**, arise from HNE adducts **2** or **3**, respectively (Chart 3). Starting from adduct **2**, cyclic hemiacetal stereoisomer **9** (6*R*,8*S*,11*R*) is the major species at equilibrium, and stereoisomer **8** (6*R*,8*R*,11*R*) is the minor

(66) Kouchakdjian, M.; Marinelli, E.; Gao, X.; Johnson, F.; Grollman, A.; Patel, D. *Biochemistry* **1989**, *28*, 5647–5657.
(67) Kouchakdjian, M.; Eisenberg, M.; Live, D.; Marinelli, E.; Grollman, A. P.; Patel, D. J. *Biochemistry* **1990**, *29*, 4456–4465.
(68) Singh, U. S.; Moe, J. G.; Reddy, G. R.; Weisenseel, J. P.; Marnett, L. J.; Stone, M. P. *Chem. Res. Toxicol.* **1993**, *6*, 825–836.
(69) Weisenseel, J. P.; Reddy, G. R.; Marnett, L. J.; Stone, M. P. *Chem. Res. Toxicol.* **2002**, *15*, 127–139.
(70) Plum, G. E.; Grollman, A. P.; Johnson, F.; Breslauer, K. J. *Biochemistry* **1992**, *31*, 12096–12102.
(71) Riggins, J. N.; Pratt, D. A.; Voehler, M.; Daniels, J. S.; Marnett, L. J. *J. Am. Chem. Soc.* **2004**, *126*, 10571–10581.
(72) Riggins, J. N.; Daniels, J. S.; Rouzer, C. A.; Marnett, L. J. *J. Am. Chem. Soc.* **2004**, *126*, 8237–8243.

species. Likewise, starting from adduct **3**, cyclic hemiacetal stereoisomer **13** (6*S*,8*R*,11S) is the major species, and stereoisomer **12** (6*S*,8*S*,11*S*) is the minor species. The stereochemistry of the cyclic hemiacetal presumably avoids steric repulsion from the large substituent groups. Detailed structural refinement of these DNA duplexes (Chart 2) containing either stereoisomers **9** or **13** is in progress.

Chemical and Biological Implications. The formation of interchain DNA cross-link of enal adducts of dG is intrinsically slow, on the order of days for the acrolein adduct and weeks for the crotonaldehyde adduct.[52,53] The formation of cyclic hemiacetals **12** and **13** (Chart 3) may, in part, explain the slower rate of interstrand cross-link formation by HNE adduct **3** in the 5′-CpG-3′ sequence.[51] The cyclic hemiacetals **12** and **13** mask the reactive aldehyde **10** necessary for formation of the interstrand 5′-CpG-3′ cross-link. Notably, HNE adduct **2** does not form interstrand cross-links in the 5′-CpG-3′ sequence,[51] despite the fact that it also undergoes ring-opening when placed opposite dC in duplex DNA, to form trace amounts of aldehyde **6**. We surmise that the explanation probably involves stereospecific differences in the conformation of aldehyde **6** as compared to that of aldehyde **10**, within the minor groove of duplex DNA. The detailed structural refinement of these DNA duplexes (Chart 2) containing either stereoisomers **9** or **13**, in progress, will be of considerable interest. The slow rate of formation of DNA−peptide conjugates by either HNE adduct **2** or **3**[58] may also be attributed to the preference for formation of cyclic hemiacetals **8** and **9**, or **12** and **13**, respectively. In fact, the four exocyclic 1,N^2-dG stereoisomers **2**−**5** arising from HNE formed DNA−peptide conjugates,[58] consistent with the observation that HNE adducts **2** and **3** undergo ring-opening to trace amounts of aldehydes **6** and **10**, and inferring that adducts **4** and **5** (Chart 1) share similar chemistry in duplex DNA.

It has been suggested that the low levels of G → T mutations observed when site-specific mutagenesis of adducts **2** and **3** was examined in mammalian cells may be attributable to the rearrangement of these adducts into the cyclic hemiacetals **8** and **9**, and **12** and **13**, respectively, because this rearrangement may facilitate formation of Watson−Crick hydrogen bonding during replication bypass of the lesions.[47] Xing et al.[73] attributed high levels of G → T mutations to the ring-closed 1,N^2-dG adducts. Similar explanations have been advanced to explain the low levels of mutations induced by the acrolein-[74,75] and crotonaldehyde-derived exocyclic 1,N^2-dG adducts,[76] as compared to the 1,N^2-propano-dG (PdG) adduct which remains in the exocyclic form.[77,78] Stein et al.[79] reported higher levels of mutations for the crotonaldehyde adducts, which may be attributable to a greater amount of the exocyclic 1,N^2-dG adducts in duplex DNA.[56] The low levels of the exocyclic 1,N^2-dG adducts, observed spectroscopically when either adducts **2** or **3** are placed opposite dC in duplex DNA, are consistent with this hypothesis. With regard to lesion bypass, DNA polymerase η cannot bypass the HNE-derived exocyclic 1,N^2-dG adducts.[80] This contrasted with its ability to bypass the less bulky acrolein-derived exocyclic 1,N^2-dG adduct,[80] suggesting that the larger HNE adducts disrupt the active site of this Y-family polymerase. However, the sequential action of human pols ι and κ was able to carry out error-free bypass and extension of the (6*S*,8*R*,11*R*) and (6*S*,8*R*,11*S*) diastereomers of the HNE adduct.[81] In this case, pol ι inserted dCTP, perhaps involving Hoogsteen pairing, and to a lesser extent dTTP opposite the HNE adduct but was unable to further elongate the primer. Further extension was observed in the presence of pol κ, which elongated from a C opposite the HNE adducts much more efficiently than when T was opposite the adducts.[81] Therefore, further conformational analyses of these HNE-derived exocyclic 1,N^2-dG adducts in both duplex DNA and in complexes with Y-family polymerases will be of interest.

Conclusions

The chemistry of the HNE-derived exocyclic 1,N^2-dG adduct **3** of (6*S*,8*R*,11*S*) stereochemistry was compared with that of the corresponding (6*R*,8*S*,11*R*) adduct **2**, when incorporated into duplex DNA. At pH 7, both stereoisomeric adducts **2** and **3** underwent ring-opening to aldehydic rearrangement products **6** and **10**, respectively, suggesting that the slow interstrand cross-link formation in DNA containing 5′-CpG-3′ sequence context by the exocyclic 1,N^2-dG adduct **3** of (6*S*,8*R*,11*S*) stereochemistry, and the lack of interstrand cross-link formation by the exocyclic 1,N^2-dG adduct **2** of (6*R*,8*S*,11*R*) stereochemistry, was not attributable to their inabilities to undergo ring-opening to reactive aldehydes **6** and **10**. Instead, these aldehydes existed in equilibrium with stereoisomeric cyclic hemiacetals **8** and **9**, and **12** and **13**. Cyclic hemiacetals **9**, arising from adduct **2**, and **13**, arising from adduct **3**, were the predominant species present at equilibrium. Cyclic hemiacetals **12** and **13** mask the reactive aldehydes **6** and **10** necessary for interstrand cross-link formation, and their presence may, in part, explain the slow interstrand cross-link formation in DNA containing 5′-CpG-3′ sequence context by the exocyclic 1,N^2-dG adduct **3** of (6*S*,8*R*,11*S*) stereochemistry.

Experimental Methods

Materials. The oligodeoxynucleotide 5′-d(GGACTCGCTAGC)-3′ was synthesized and purified by anion-exchange chromatography by the Midland Certified Reagent Co. The oligonucleotides containing HNE-derived exocyclic 1,N^2-dG adducts **2** and **3** in the dodecamer 5′-d(GCTAGCXAGTCC)-3′, where X represents the HNE-dG adducts, were synthesized, purified, and characterized as reported.[50,51] The purities of the adducted oligodeoxynucleotides were assessed by capillary gel electrophoresis and HPLC. Oligodeoxynucleotides were desalted by chromatography on Sephadex G-25.

Mass Spectrometry of the HNE Adducts in Duplex Oligodeoxynucleotides. The duplex oligodeoxynucleotides containing either stereoisomeric HNE adducts **2** or **3** were analyzed by mass spectrometry. The concentrations of the oligonucleotides were determined by UV absorption at 260 nm, and the extinction coefficients of both sequences were calculated as 1.12×10^5 L mol^{-1} cm^{-1}.[82] The strands were annealed in buffer containing 10

(73) Xing, D. X.; Sun, L. X.; Cukier, R. I.; Bu, Y. X. *J. Phys. Chem. B* **2007**, *111*, 5362–5371.
(74) VanderVeen, L. A.; Hashim, M. F.; Nechev, L. V.; Harris, T. M.; Harris, C. M.; Marnett, L. J. *J. Biol. Chem.* **2001**, *276*, 9066–9070.
(75) Yang, I. Y.; Hossain, M.; Miller, H.; Khullar, S.; Johnson, F.; Grollman, A.; Moriya, M. *J. Biol. Chem.* **2001**, *276*, 9071–9076.
(76) Fernandes, P. H.; Kanuri, M.; Nechev, L. V.; Harris, T. M.; Lloyd, R. S. *Environ. Mol. Mutagen.* **2005**, *45*, 455–459.
(77) Moriya, M.; Zhang, W.; Johnson, F.; Grollman, A. P. *Proc. Natl. Acad. Sci. U.S.A.* **1994**, *91*, 11899–11903.
(78) Moriya, M.; Pandya, G. A.; Johnson, F.; Grollman, A. P. *IARC Sci. Publ.* **1999**, *150*, 263–270.
(79) Stein, S.; Lao, Y.; Yang, I. Y.; Hecht, S. S.; Moriya, M. *Mutat. Res.* **2006**, *608*, 1–7.
(80) Minko, I. G.; Washington, M. T.; Kanuri, M.; Prakash, L.; Prakash, S.; Lloyd, R. S. *J. Biol. Chem.* **2003**, *278*, 784–790.
(81) Wolfle, W. T.; Johnson, R. E.; Minko, I. G.; Lloyd, R. S.; Prakash, S.; Prakash, L. *Mol. Cell. Biol.* **2006**, *26*, 381–386.
(82) Cavaluzzi, M. J.; Borer, P. N. *Nucleic Acids Res.* **2004**, *32*, e13.

mM NaH_2PO_4, 100 mM NaCl, and 50 μM Na_2EDTA (pH 7.0). The solution containing the modified and complementary oligodeoxynucleotides at 1:1 stoichiometry was heated to 95 °C for 10 min, then slowly cooled to room temperature. The duplex DNA was purified by DNA-grade hydroxylapatite chromatography with a gradient from 10 to 200 mM NaH_2PO_4 in 100 mM NaCl, 50 μM Na_2EDTA (pH 7.0), and then desalted by Sephadex G-25. The duplexes were identified by MALDI-TOF mass spectroscopy on Voyager-DE STR spectrometer (Applied Biosystems, Inc.). The oligodeoxynucleotide duplex was dissolved in distilled water or 50 mM NaCl to form a 0.5 mM strand concentration solution. One microliter of the oligodeoxynucleotide duplex solution was combined with 1 μL of hydroxypicolinic acid matrix solution and dried at room temperature.

The MALDI-TOF mass spectrum of the duplex oligodeoxynucleotide containing stereoisomer **2** showed a mass for the modified strand of *m*/*z* 3801.9 (calcd for M − H, 3800.9), and a mass of *m*/*z* of 3645.4 for the complementary strand (calcd for M − H, 3645.4). A mass of *m*/*z* of 3824.8 was observed for the modified strand (calcd for M + Na − 1, 3823.9) in 50 mM NaCl solution. The complementary strand was observed at *m*/*z* of 3647.0. The MALDI-TOF mass spectrum of the duplex oligodeoxynucleotide containing stereoisomer **3** showed a mass for the modified strand of *m*/*z* 3803.8 (calcd for M − H, 3800.9), a mass of *m*/*z* 3645.2 for the complementary strand (calcd for M − H, 3645.4). A mass corresponding to the duplex containing **3** at *m*/*z* 7451.0 (calcd for M − H, 7447.3) was also observed. A mass of *m*/*z* 3802.7 was observed for the modified strand in 50 mM NaCl solution. The complementary strand was observed at *m*/*z* 3646.4.

NMR. Samples were at 1.0 mM strand concentration. Samples for the nonexchangeable protons were dissolved in 280 μL of a buffer containing 10 mM NaH_2PO_4, 100 mM NaCl, 50 μM Na_2EDTA (pH 7.0). They were exchanged with D_2O and suspended in 280 μL of 99.996% D_2O. The pH was adjusted to 7.0 with dilute DCl or NaOD solutions. Samples for the observation of exchangeable protons were dissolved in 280 μL of 10 mM NaH_2PO_4, 100 mM NaCl, 50 μM EDTA (pH 7.0) containing 9:1 H_2O/D_2O (v/v), and the pH was adjusted to 7.0. NMR experiments were performed on a Bruker Avance 800 spectrometer with a cryogenic probe (Bruker Instruments). The temperature was 25 °C for observation of the nonexchangeable protons and 5 °C for observation of the exchangeable protons. Chemical shifts for ^1H were referenced to water. Data were processed using FELIX 2000 (Accelrys, Inc.) on Silicon Graphics workstations (Silicon Graphics, Inc.). For all NMR experiments, a relaxation delay of 1.5 s was used. Two-dimensional homonuclear NMR spectra were recorded with 512 real data in the t2 dimension and 2048 real data in the t1 dimension. NOESY spectra were zero-filled during processing to create a matrix of 1024 × 1024 real points, and other spectra were zero-filled to create a matrix of 1024 × 512 real points. A skewed sinebell-square apodization with 15° phase shift was used in both dimensions to process COSY spectra. The total correlation spectroscopy mixing time was 80 ms for the duplex containing stereoisomer **2** and 100 ms for the duplex containing stereoisomer **3**. For assignment of exchangeable protons, NOESY experiments used the watergate sequence.[83] The mixing time was 250 ms. For assignment of nonexchangeable protons and the derivation of distance restraints, NOESY experiments used TPPI quadrature detection and mixing times of 60 and 250 ms were used. DQF-COSY experiments were performed with TPPI quadrature detection and presaturation of the residual water during the relaxation delay.

Acknowledgment. Dr. Markus Voehler assisted with NMR experiments. Drs. Constance M. Harris and Thomas M. Harris provided thoughtful comments regarding the chemistry of these adducts. This work was supported by NIH Grant ES-05355 (C.J.R. and M.P.S.). The Vanderbilt University Center in Molecular Toxicology is supported by NIH Grant P30 ES-00267.

JA801824B

(83) Piotto, M.; Saudek, V.; Sklenar, V. *J. Biomol. NMR* **1992**, *2*, 661–665.